Available online at www.sciencedirect.com
ScienceDirect
Journal of Molecular Catalysis A: Chemical 256 (2006) 149–155
JOURNAL OF MOLECULAR CATALYSIS A: CHEMICAL
www.elsevier.com/locate/molcata

Heterolytic dissociation and recombination of H_2 over Zn,H-ZSM-5 zeolites—A density functional model study

Hristiyan A. Aleksandrov [a], Georgi N. Vayssilov [a,*], Notker Rösch [b]

[a] *Faculty of Chemistry, University of Sofia, 1126 Sofia, Bulgaria*
[b] *Department Chemie, Technische Universität München, 85747 Garching, Germany*

Received 27 February 2006; received in revised form 13 April 2006; accepted 22 April 2006
Available online 5 June 2006

Abstract

This computational study aims at clarifying which type of cationic Zn species in Zn,H-ZSM-5 zeolite are suitable catalytic sites for H_2 dissociation and which for the recombination and desorption of H_2. The latter processes, crucial for the dehydrogenation of alkanes over such zeolites, are assumed to involve Zn species. We described heterolytically dissociated H_2 on four types of zeolite-supported Zn species by applying a density functional method to suitable cluster models. We determined the dissociation of hydrogen on Zn^{2+} species to be exothermic (by 14 and 30 kJ/mol, depending on the model). Corroborating this result, the calculated vibrational frequencies of the Zn–H bond of such Zn^{2+} complexes, 1935 and 1943 cm^{-1}, agree well with experimental values for dissociatively adsorbed H_2 at Zn-containing H-ZSM-5 zeolite, 1934–1936 cm^{-1}. Due to the preference for H_2 dissociation, bare Zn^{2+} species in zeolite are not considered as catalytic sites for H_2 recombination. However, if an additional OH^- or H_2O ligand is coordinated at a Zn^{2+} center, H_2 recombination becomes exothermic. Thus, $Zn(H_2O)^{2+}$ and $ZnOH^+$ species in Zn-exchanged zeolites are suggested to be involved in the dehydrogenation of alkanes over Zn,H-ZSM-5.

Keywords: Zinc species; Zeolites; Dihydrogen; Zn–H frequency

1. Introduction

Zn-exchanged H-ZSM-5 zeolites are efficient catalysts for the dehydrogenation and the aromatization of alkanes [1–3]. Analyzing the mechanism of propane aromatization, Biscardi and Iglesia [4,5] proposed that initial C–H bond cleavage occurs on Brønsted acid sites of the zeolite whereas Zn species participate in the subsequent recombination and desorption of H_2. Hence, understanding dissociation and recombination processes of H_2 on Zn,H-ZSM-5 zeolites is important for clarifying the mechanism of alkane dehydrogenation. Kazansky et al. [6–8] considered experimentally the dissociation of H_2 on Zn,H-ZSM-5 and assigned a signal at 1934–1936 cm^{-1} to the IR vibrational frequency of Zn–H bonds. Studying Zn,H-ZSM-5 with high Si/Al ratios, 25 and 41, prepared by three different techniques (ion-exchange, incipient wetness impregnation, and reaction of the protonic form H-ZSM-5 with zinc vapor at high temperature −773 K), they concluded that the properties of Zn,H-ZSM-5 strongly depend on the preparation method. Because they found a strong Zn–H signal only for the sample prepared by the third method, they suggested that H_2 can be dissociated only on partially charge compensated Zn^{2+} ions, i.e. on Zn^{2+} ions which are located close to only one Al center, while the second Al center lies at a larger distance. Such partially compensated (and more reactive) Zn^{2+} ions are assumed to be formed only by reaction with Zn vapor, whereas under the other conditions an additional charge-compensating O-containing ligand is coordinated to Zn^{2+}.

To check this hypothesis, Shubin et al. [9,10] and Yakovlev et al. [11] modeled H_2 adsorption at Zn^{2+} with zeolite cluster models where one Al center was located in each of two adjacent five-membered rings. Applying different density functionals (BP at the HF geometry [10], B3LYP [9], PW at the LDA geometry [11]) to several isolated cluster models, they calculated molecular and dissociative adsorption of H_2 to be exothermic, by −32 kJ/mol [9] and −178 kJ/mol [9] to −138 kJ/mol [11], respectively. For a completely charge compensated Zn^{2+} ion,

* Corresponding author.
E-mail addresses: gnv@chem.uni-sofia.bg (G.N. Vayssilov), roesch@ch.tum.de (N. Rösch).

1381-1169/$ – see front matter © 2006 Elsevier B.V. All rights reserved.
doi:10.1016/j.molcata.2006.04.051

that interacted simultaneously with two Al centers of one zeolite ring, the reaction energy for heterolytic dissociation was determined between −29 kJ/mol [11] and 5 kJ/mol [10]. In a detailed study of H_2 adsorption on various metal cations in MOR zeolite, using a periodic supercell density functional (DF) approach and the PW exchange-correlation functional, Benco et al. [12] calculated H_2 dissociation to be exothermic on completely or partially compensated Zn^{2+} sites, by −52 and −116 kJ/mol, respectively.

Employing a similar computational approach, Barbosa and van Santen [13] considered adsorption and dissociation of H_2 on yet another Zn species, namely $ZnOZn^{2+}$. They determined a small adsorption energy of H_2, −6 to −11 kJ/mol, and significantly larger energies for dissociative adsorption, −30 to −118 kJ/mol; in all cases, $ZnOZn^{2+}$ species are decomposed to ZnH^+ and $ZnOH^+$ cationic species. Hence, the process of dissociation of H_2 on Zn,H-ZSM-5 strongly depends on the type of the Zn species in the pores of ZSM-5 zeolite.

However, all these computational studies modeled the interaction of hydrogen only with Zn^{2+} and $ZnOZn^{2+}$ species, but not with $ZnOH^+$ and $Zn(H_2O)^{2+}$, which we recently determined to be the most stable Zn-containing species in Zn,H-ZSM-5 [14]. In addition, several experimental works suggested that $ZnOH^+$ species are the catalytically active centers for alkane dehydrogenation and aromatization [1,4,5,15]. As a comprehensive

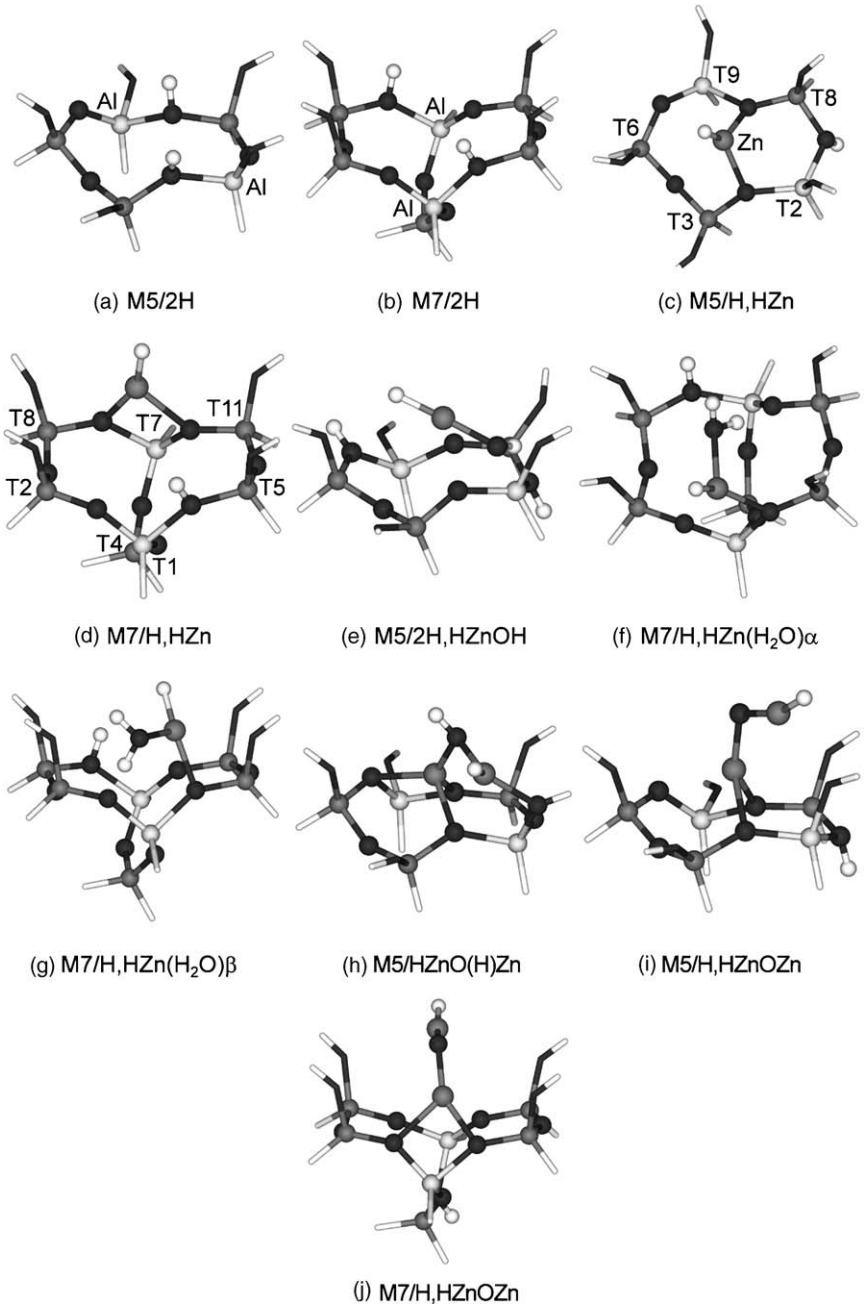

Fig. 1. Optimized structures of protonic forms of both zeolite rings, (a) M5/2H and (b) M7/2H, and structures of different Zn species with dissociated H_2: (c) M5/H,HZn, (d) M7/H,HZn, (e) M5/2H,HZnOH, (f) M7/H,HZn(H_2O)α, (g) M7/H,HZn(H_2O)β, (h) M5/HZnO(H)Zn, (i) M5/H,HZnOZn, and (j) M7/H,HZnOZn.

theoretical study of the reactivity of all types of Zn species with molecular hydrogen is lacking, there is still no a clear picture of the role of Zn species in the dehydrogenation of alkanes.

In a preceding computational study [14], we considered the structure and stability of four Zn species – Zn^{2+}, $ZnOH^+$, $Zn(H_2O)^{2+}$, and $ZnOZn^{2+}$ – on two zeolite fragments M5 and M7, which each comprise two Al centers among five and seven T atoms, respectively (Fig. 1a and b). For these cluster models, we determined $Zn(H_2O)^{2+}$ to be the most stable Zn species. For example, it was calculated about 50 kJ/mol more stable than a structure containing $ZnOH^+$ and a bridging zeolite OH group. The calculated structural parameters of both $Zn(H_2O)^{2+}$ and $ZnOH^+$ species agreed well with available EXAFS results [1,5]. We also determined the formation of $ZnOZn^{2+}$ from $ZnOH^+$ or $Zn(H_2O)^{2+}$ to be energetically unfavorable, in agreement with previous studies using similar or larger zeolite fragments [11,16,17]. In addition, the EXAFS spectra [1,5] do not show close Zn–Zn contacts, thus providing further evidence for the absence of $ZnOZn^{2+}$ species in catalytically active Zn-containing zeolite samples.

In the following, we report a systematic study on the dissociation or recombination of H_2 at the four types of Zn species described above. From the calculated reaction energies for these models, one can identify, on the one hand, which Zn species favor recombination of H_2, hence ultimately, which sites might be involved in the second step of alkane dehydrogenation. On the other hand, the obtained results can be related to H_2 dissociation observed experimentally on some Zn,H-ZSM-5 samples. Pursuing the latter issue, we also calculated vibrational frequencies of Zn–H bonds for all adsorption complexes, to gather further evidence from a comparison with available experimental data [6,8].

2. Methods and models

The calculations were carried out with the linear combination of Gaussian-type orbitals fitting-functions density functional method (LCGTO-FF-DF) [18] as implemented in the program ParaGauss [19,20]. We used the gradient-corrected exchange-correlation functional proposed by Becke and Perdew [21]. We represented the Kohn–Sham orbitals by Gaussian-type basis sets, which were contracted in generalized form: (6s1p) → [4s1p] for H, (9s5p1d) → [5s4p1d] for O, (12s9p2d) → [6s4p2d] for Al and Si [22], (15s11p6d) → [6s5p3d] for Zn [23]. The auxiliary basis set used in the LCGTO-FF-DF method to describe the Hartree part of the electron–electron interaction was derived from the orbital basis set in the usual fashion [18] and augmented by five p-type and five d-type "polarization" exponents for each atom. These exponents were constructed as geometric series with a factor 2.5, starting with 0.1 and 0.2 for p- and d-exponents, respectively [18,24].

Initially, we optimized the MFI structure at the molecular mechanical (MM) level with the program GULP [25], using a previously reported shell model force field (FF) [26,27]. From this structure we chose two model clusters M5 and M7, to be treated at the quantum mechanical level (QM). These models, representing one and two coupled five-membered zeolite rings, respectively, include the crystallographic positions T2–T3–T6–T9–T8 and T8–T7–T11–T5–T1–T2–T4, respectively. Both zeolite fragments, M5 and M7, face the main channel of the MFI structure as five- and six-membered rings, respectively (Fig. 1a and b). Each cluster contains two Al centers, located at the positions T2 and T9 in model M5 and at the positions T1 and T7 in model M7 (Fig. 1a and b). We chose these computational models to investigate the influence of the coordination position and the cluster size on the stability of the Zn species and on their preference for recombination of dissociated H_2. Zeolite rings with such size had been suggested as preferred positions for Zn^{2+} after extensive computational studies [16,17] which modeled the location of divalent metal cations at eight coordination positions in zeolite MFI.

The dangling bonds at the boundary of the model clusters were saturated by H atoms, and the directions of these bonds were kept fixed as obtained in the MM model. The initial structures of the cluster models were determined in a two-step process. First, the lengths of the dangling T–H or O–H bonds were optimized while keeping the positions of all other atoms of the cluster fixed; in the second step, the remaining structure of the cluster was optimized, keeping the positions of all saturating H atoms fixed as obtained in the first step. In subsequent geometry optimizations, both of protonic and Zn-containing models, only the positions of the oxygen centers of the ring, the protons of the bridging OH groups, and the guest species were relaxed. This step-wise strategy yields reliable structures and characteristic vibrational frequencies, as was concluded by comparing results from calculations on various metal complexes and other species in zeolites [28] to pertinent experimental data.

The results of the initial optimizations of the four types of Zn species in both zeolite fragments, M5 and M7, have previously been reported [14] and shortly described in the Introduction. In the present study, for each type of species, we modeled structures that represent a dissociated state of H_2. For this purpose, we added to each cluster model one H^- moiety, coordinated to the Zn ion, and one proton which was allowed to interact either with a basic zeolite O center or, where available, an O center of the Zn species. In all cases we selected structures where both hydrogen ions, H^+ and H^-, were suitably located for recombination to H_2.

After geometry optimization of the model clusters, all vibrational frequencies of the guest moiety were evaluated in the harmonic approximation. The force constants of the vibrational modes were obtained numerically as finite differences of analytical energy gradients. To calibrate our calculated IR frequencies of Zn–H bonds, we also calculated Zn–H frequencies of small zinc species containing a Zn–H bond – H–Zn, H–ZnOH, H–ZnH, H–ZnZn, and H–ZnCl – and we compared our results with available experimental data (Table 1) [29,30]. For these test species, the average difference between our calculated results and the Zn–H IR bands measured by Wang and Andrews [29] is 35 cm^{-1}, while for the results measured by Macrae et al. [30] that difference is 41 cm^{-1} [31]. The overall average deviation between our calculated results for these test Zn species and the corresponding experimental data is 38 ± 15 cm^{-1}. Thus, we applied a correctional shift of -38 cm^{-1} to our calculated

Table 1
Calculated and experimental IR frequencies and their differences Δ (cm^{-1}) of Zn—H bonds for some small species

	Calculated	Experimental		Δ[a]		α[b]	
		Set 1[c]	Set 2[d]	Set 1[c]	Set 2[d]	Set 1[c]	Set 2[d]
H–Zn	1526	1494	1499	32	27	0.9790	0.9823
H–ZnOH	2012	1955		57		0.9717	
H–ZnH	1918, 1926	1870	1881	48, 56	37, 45	0.9750, 0.9709	0.9807, 0.9766
H–ZnZn	1678		1648		30		0.9821
H–ZnCl	1963	1952		11		0.9944	

Also shown are the corresponding scaling factors α (see text).
[a] Average $\Delta = 38 \pm 15\ cm^{-1}$.
[b] Average $\alpha = 0.9768$.
[c] Ref. [30].
[d] Ref. [29].

results; the frequency values displayed in Table 2 have been corrected in this way. From the same set of experimental and calculated data (Table 1), one can alternatively derive a scaling factor of 0.9768, to be applied to the calculated Zn–H vibrational frequencies. With this scaling factor, one obtains Zn–H frequencies for the zeolite models, which are 6–8 cm^{-1} smaller than those determined by the "shift" procedure used in the following.

3. Results and discussion

3.1. Structures

The optimized structures of the Zn-containing cluster models with dissociatively adsorbed hydrogen are shown in Fig. 1c–j. In Table 2, we report selected interatomic distances.

Heterolytic H_2 adsorption on Zn^{2+} cations at both zeolite models M5 and M7 results in the formation of ZnH^+ species which are coordinated to two basic O centers. In M5/H,HZn (Fig. 1c), these two O atoms are bound to two different Al centers and the Zn–O_z distances are almost equal, 205 and 208 pm. Yakovlev et al. [11] also found two Zn–O_z contacts for ZnH^+ species at five-membered zeolite rings; they reported Zn–O distances that are 7 pm shorter than those of the present study, inline with experience the local density approximation (LDA), employed in that work, often underestimates bond distances [32]. In the larger model, M7/H,HZn (Fig. 1d), ZnH^+ is located at one of the Al centers, while the other Al center is compensated by a proton. This difference in coordination of the Zn^{2+} species at the two zeolite fragments was not observed for the initial M5/Zn and M7/Zn complexes, where the zinc ion has three close contacts with zeolite oxygen atoms bound to both Al centers [14].

Next, we modeled dissociatively adsorbed H_2 on $ZnOH^+$ species at both zeolite fragments. In the optimized structure M5/2H,HZnOH (Fig. 1e), a neutral moiety HZnOH is formed which is bound to the zeolite cluster only by a hydrogen bond with $R(H–O_z) = 184$ pm. The corresponding structure of an M7 model, constructed initially as M7/2H,HZnOH, was transformed during geometry optimization into the complex M7/H,HZn(H_2O), as a zeolite proton migrated to the O center of the guest species. This finding is reminiscent of our earlier results for the initial complexes M5/H,ZnOH and M7/H,ZnOH, where the corresponding $Zn(H_2O)^{2+}$ forms were more stable than $ZnOH^+$ in the vicinity of a bridging OH group [14].

Table 2
Selected interatomic distances (pm) and shifted vibration frequencies[a] of the Zn—H mode (cm^{-1}) calculated for various model clusters

Model	O_z–H	Zn–O_z	Zn–O[b]	O—H[b]	H_w–O_z	Zn—H	Frequency[a]
M5/H,HZn	98	208[c]/205[d]				152	1935
M7/H,HZn	98	198, 214[e]				152	1943
M5/2H,HZnOH	98, 98		178		184	151	1946
M5/H,HZn(H_2O)α	–	200[c]/196[d]	204	105, 100	155, 191	205, 214	
M5/H,HZn(H_2O)β	98	201[f]/210[d]	438	103, 98	155	153	
M7/H,HZn(H_2O)α	98	204, 231[f]	212	101, 97	167	154	1871
M7/H,HZn(H_2O)β	98	201[f]	212	100, 98	176	154	1878
M5/HZnO(H)Zn	–	204, 215[c]/192, 226[d]	190, 202	97		154	1874
M5/H,HZnOZn	98	214[c]/200[d]	179, 181			153	1907
M7/H,HZnOZn	98	197, 220[f]	178, 179				1958

[a] See text for the correction procedure; IR vibration frequency of Zn—H in Zn,H-ZSM-5 zeolite measured at 1934–1936 cm^{-1}, Refs. [6,8].
[b] Distances within the guest species.
[c] Distance involving an O center bound to Al at T2.
[d] Distance involving an O bound to Al at T9.
[e] Distance involving an O center bound to Al at T7.
[f] Distance involving an O center bound to Al at T1.

Table 3
Reaction energies (kJ/mol) of hydrogen dissociation on different Zn-containing species

Model reactions	$k=5$	$k=7$
Mk/Zn + H_2 → Mk/H,HZn	−14	−30
Mk/H,ZnOH + H_2 → Mk/2H,HZnOH	84	–
Mk/Zn(H_2O) + H_2 → Mk/H,HZn(H_2O)	−2	15
Mk/ZnOZn + H_2 → Mk/H,HZnOZn	93	48
Mk/ZnOZn + H_2 → Mk/HZnO(H)Zn	−129	0[a]

Negative values represent exotermic processes.
[a] Optimization always lead to recombination of H^+ and H^- to molecular H_2 as H^- and H^+ are initially located at neighboring centers.

Here, we calculated the heterolytic dissociative adsorption of H_2 on the complex with $Zn(H_2O)^{2+}$ species, M5/H,HZn(H_2O), to be less stable than the initial M5/Zn(H_2O) complex and an isolated H_2 molecule. In an attempt to model heterolytic adsorption, we observed that either H_2 recombines and desorbs, or, if this is not possible, the water molecule leaves the complex (not shown in Fig. 1). The latter optimized structure is 89 kJ/mol less stable than the separated reactants. At the larger model cluster, M7/H,HZn(H_2O), we considered four different initial structures, two of them were found to be stable minima (Fig. 1f and g). In both structures, the Zn ion is located close to one of the Al centers and one hydrogen atom of H_2O forms a hydrogen bond with the zeolite framework (Table 2). However, H_2 dissociation is endothermic for both these structures of the larger model (Table 3).

In the case of $ZnOZn^{2+}$ species, H^+ formed by (formally) dissociated H_2 can be located either on the O center of the $ZnOZn^{2+}$ species, modeled as M5/HZnO(H)Zn (Fig. 1h), or on an O center of the zeolite fragment, modeled as M5/H,HZnOZn (Fig. 1i). The former structure M5/HZnO(H)Zn was found 222 kJ/mol more stable than the second one. In the complex M5/HZnO(H)Zn, one of the Zn ions is located in the center of the zeolite five-ring while the other Zn ion, interacting with H^-, is coordinated to a border O center. In both structures at the M7 zeolite fragment, M7/H,HZnOZn and M7/HZnO(H)Zn, H^+ and H^- recombined to H_2 during the geometry optimization. To estimate the energy difference between desorbed H_2 and H_2 adsorbed dissociatively at the model M7/ZnOZn, we also calculated an alternative structure M7/H,HZnOZn where H^+ and H^- are not located close each other, to avoid recombination (Fig. 1j); that structure is 48 kJ/mol less stable than the initial M7/ZnOZn structure and H_2. Optimization of the other structure with H^+ located at the $ZnOZn^{2+}$ moiety, M7/HZnO(H)Zn, and H^- attached to neighboring centers always lead to recombination.

3.2. Energetics

In Table 3 we report the reaction energies for heterolytic dissociation of H_2 on different Zn species, calculated with respect to an isolated H_2 molecule and the initial Zn-containing structure. For the Zn^{2+} species the dissociation of H_2 molecule to H^+ and H^- is exothermic with −14 and −30 kJ/mol at M5 and M7 clusters, respectively. In contrast, at Zn species containing an additional ligand, $ZnOH^+$ and $Zn(H_2O)^{2+}$, recombination and desorption of H_2 is energetically preferred.

The position of $ZnOZn^{2+}$ moieties in the zeolite framework determines the preference of these species for dissociation or recombination. At M5, we calculated dissociation to be strongly exothermic, −129 kJ/mol (Table 3). Barbosa et al. considered H_2 dissociation on $ZnOZn^{2+}$ species sorbed at 5T cluster model [33] and CHA frameworks using periodic slab models [13]. They found that the reaction is exothermic and in the latter case leads to the decomposition of $ZnOZn^{2+}$ species into $ZnOH^+$ and ZnH^+ moieties. A similar finding was reported for H_2 adsorption on $ZnOZn^{2+}$ species bound simultaneously to two adjacent five-rings of MFI [11]. These results are in line with our findings for the M5 cluster model (see above). However, our calculations did not indicate that $ZnO(H)Zn^+$ species decompose, likely due to the limited size of the zeolite model M5. On $ZnOZn^{2+}$ species located at the larger cluster model M7, we found the opposite trend: H^+ and H^- recombine to H_2 that desorbs from the cluster. Note, however, that according to our previous work [14] as well as other experimental and computational studies [1,5,11,17], $ZnOZn^{2+}$ species are unlikely to exist in zeolite cavities. The formation of such species was calculated to be unfavorable also with a larger zeolite fragment which contained two five-rings [11].

3.3. Vibrational frequencies

We also calculated the Zn–H vibrational frequency of the modeled complexes to check when this frequency is close to the experimental values for H_2 dissociated on Zn,H-ZSM-5 samples [6,8], 1934–1936 cm^{-1} (Table 2). As described in Section 2, the calculated frequencies of Table 2 have been corrected by a constant shift of −38 cm^{-1}. The Zn–H frequencies of both structures with Zn^{2+} species, 1935 and 1943 cm^{-1} (Table 2), agree best with the experimental results; this provides further evidence that H_2 dissociated heterolytically on Zn^{2+} cations without additional ligands is observed in the experiment. Calculated Zn–H vibrational frequencies of most of the other complexes differ significantly from the experimental values (Table 2) while the Zn–H frequency of M5/2H,HZnOH (Fig. 1e), 1946 cm^{-1}, is also close to experiment. However, the heterolytic dissociation of H_2 in this latter complex is endothermic, by 84 kJ/mol; thus, such species are unlikely to be formed. One reaches the same conclusions when one bases the comparison on the scaled values of the Zn–H frequencies (see above).

4. Discussion

As mentioned in Section 1, the present work has two goals:

(i) on the base of energetic arguments, identify Zn species that are able to dissociate heterolytically H_2 as well as compare calculated and experimental vibrational frequencies of Zn–H bonds;
(ii) identify Zn species, on which the recombination of heterolytically dissociated H_2 is energetically favorable, to

select sites that may possibly assist the step of hydrogen recombination during the alkane dehydrogenation.

The following discussion addresses these two problems on the basis of obtained computational results.

4.1. Dissociative adsorption of H_2 on Zn^{2+} species

Kazansky et al. [6,8] proposed that Zn^{2+}, when partially charge compensated (by only one Al center), are the most reactive species in the pores of ZSM-5 and that only these species are able to dissociate hydrogen. Indeed, several computational studies [9,11,12] demonstrated that partially compensated Zn^{2+} species (when the second Al center is located in a neighboring zeolite ring or farther away in the zeolite framework) are very reactive towards heterolytic dissociation of H_2. Employing the exchange-correlation approximations B3LYP and PW, the latter at an LDA geometry as well as in a periodic supercell calculation, the reaction was found to be exothermic by −178 kJ/mol [9], −138 kJ/mol [11], and −116 kJ/mol [12], respectively. However, such Zn^{2+} species bound close to only one Al center are unlikely to exist in zeolite cavities because a large electrostatic energy would have to be overcome during their formation, ∼200 kJ/mol, when the distance between the Al centers is 900 pm or more [34]. Even if partially compensated Zn^{2+} species could be produced in the absence of water, as in the exchange reaction with zinc vapor [6], these species are not expected to be active in the recombination of H_2 because the process on them is far too endothermic.

However, heterolytic dissociation of H_2 is exothermic not only on partially compensated Zn^{2+}, but also on completely compensated Zn^{2+} species; reaction energies depend on the model and method used: −29 kJ/mol [11] or −30 to −14 kJ/mol calculated in the present work (Table 3). Recent plane-wave calculations [12] suggest an even larger exothermicity of this process, −52 kJ/mol. Therefore, Kazansky et al. [6,8] may actually have observed H_2 dissociation on normal, completely compensated Zn species in the sample prepared by Zn vapor deposition. Further support for this conclusion can be derived from our results for the Zn–H frequencies, 1935 and 1943 cm^{-1} (Table 2), calculated for the complexes with H_2 dissociated on the models which contain completely compensated Zn^{2+} species, M5/H,HZn and M7/H,HZn; the corresponding frequencies fit very well the experimental IR values, 1934–1936 cm^{-1} [6,8].

As discussed in Section 1, the preparation method influences the properties of Zn,H-ZSM-5 samples. The material, which was experimentally demonstrated to be catalytically active, is produced by incipient wetness impregnation or by ion-exchange [1,4,5]. In these preparation methods, the cationic Zn species contain additional ligands, e.g. OH^- or H_2O [1,5,15]. According to our present results, such $ZnOH^+$ or $Zn(H_2O)^{2+}$ species are inactive in the heterolytic dissociation of H_2. This agrees with the experimental observation [6] that the Zn–H vibration mode does not occur in the IR spectra of the samples prepared by ion-exchange and incipient wetness impregnation. The band is detected only on Zn,H-ZSM-5 samples prepared by reacting the protonic form H-ZSM-5 with zinc vapor at high temperature.

4.2. Recombination of dissociatively adsorbed hydrogen

According to Biscardi and Iglesia [1,4,5], Zn species should facilitate the second stage of the dehydrogenation of alkanes when the recombination of H^+ and H^- to H_2 is *exothermic*. Therefore, we are looking for structures where the heterolytic dissociation of H_2 is *endothermic*.

From our previously reported computational results [14], we concluded that $Zn(H_2O)^{2+}$ are the most stable Zn species at zeolite rings which contain two Al centers. As found here, recombination and desorption of H_2 is energetically favored on such sites and on $ZnOH^+$. Thus, these latter complexes are candidates for sites that can assist in the hydrogen recombination step. Despite a number of theoretical studies on Zn-containing species in ZSM-5 zeolite [9–13,33], no active centers had previously been suggested that would be suitable in the catalytic recombination of hydrogen. The present theoretical results allow us to discriminate the potential catalytic effect of Zn^{2+} species favoring H_2 dissociation on the one hand, and of $ZnOH^+$ and $Zn(H_2O)^{2+}$ species that favor recombination and desorption of H_2, on the other hand.

Although $Zn(H_2O)^{2+}$ complexes are found to favor H_2 recombination (Table 3), these species may not be active catalytic sites for alkane dehydrogenation as this latter process occurs at high temperatures where the H_2O ligand might desorb. This, in turn, would lead to the formation of Zn^{2+} species [1,35] which prevent H_2 recombination (Table 3). Thus, one is lead to conclude that the only type of cationic zinc species active in H_2 recombination at high temperature is $ZnOH^+$.

5. Conclusions

Using DF (BP86) calculations on various cluster models, we checked which type of Zn species in ZSM-5 zeolite are potential catalytic sites for the heterolytic dissociation of H_2 and which for the recombination of heterolytically dissociated H_2. This latter process has been suggested to be the second step of the alkane dehydrogenation [4,5]. We modeled dissociatively adsorbed hydrogen on different Zn species – Zn^{2+}, $ZnOH^+$, $Zn(H_2O)^{2+}$, and $ZnOZn^{2+}$ – and found dissociation of hydrogen to be exothermic on Zn^{2+} species. These results are in line with those of several previous investigations [11,12], including also experimental observations of Zn–H vibrational bands [6,8] that essentially coincide with the corresponding frequencies simulated here for M5/H,HZn and M7/H,HZn structures. Consequently, Zn^{2+} species in ZSM-5 zeolite are suitable for H_2 dissociation, but not as catalysts for the recombination of hydrogen. In contrast, an additional ligand coordinated at Zn^{2+} species, such as OH^- or H_2O, renders recombination of H_2 exothermic. Therefore, our results suggest that $Zn(H_2O)^{2+}$ and $ZnOH^+$ species should be able to catalyze the second step of alkane dehydrogenation. However, as dehydrogenation is accomplished at high temperature where the H_2O ligand of $Zn(H_2O)^{2+}$ can desorbed, $ZnOH^+$ remain as the only species active in the recombination of H_2 at the commonly used high reaction temperature.

The results of the present systematic computational exploration of pertinent models allowed us to rationalize the catalytic

role of different Zn-containing species in zeolites. Our study is the first computational work that considered the recombination of H_2 on the pertinent species $Zn(H_2O)^{2+}$ and $ZnOH^+$ in zeolites.

Acknowledgments

This work was supported by Deutsche Forschungsgemeinschaft, the Nanouniverse project and National Science Fund (Bulgaria), Alexander von Humboldt Foundation, and Fonds der Chemischen Industrie (Germany).

References

[1] J.A. Biscardi, G.D. Meitzner, E. Iglesia, J. Catal. 179 (1998) 192–202.
[2] J. Heemsoth, E. Tegeler, F. Roessner, A. Hagen, Micropor. Mesopor. Mater. 46 (2001) 185–190.
[3] A. Hagen, E. Schneider, M. Benter, A. Krogh, A. Kleinert, F. Roessner, J. Catal. 226 (2004) 171–182.
[4] J.A. Biscardi, E. Iglesia, J. Catal. 182 (1999) 117–128.
[5] J.A. Biscardi, E. Iglesia, Phys. Chem. Chem. Phys. 1 (1999) 5753–5759.
[6] V.B. Kazansky, A.I. Serikh, Phys. Chem. Chem. Phys. 6 (2004) 3760–3764.
[7] V.B. Kazansky, J. Catal. 216 (2003) 192–202.
[8] V.B. Kazansky, A.I. Serikh, B.G. Anderson, R.A. van Santen, Catal. Lett. 88 (2003) 211–217.
[9] A.A. Shubin, G.M. Zhidomirov, V.B. Kazansky, R.A. van Santen, Catal. Lett. 90 (2003) 137–142.
[10] A.A. Shubin, G.M. Zhidomirov, A.L. Yakovlev, R.A. van Santen, J. Phys. Chem. B 105 (2001) 4928–4935.
[11] A.L. Yakovlev, A.A. Shubin, G.M. Zhidomirov, R.A. van Santen, Catal. Lett. 70 (2000) 175–181.
[12] L. Benco, T. Bucko, J. Hafner, H. Toulhoat, J. Phys. Chem. B 109 (2005) 22491–22501.
[13] L.A.M.M. Barbosa, R.A. van Santen, J. Phys. Chem. B 107 (2003) 14342–14349.
[14] H.A. Aleksandrov, G.N. Vayssilov, N. Rösch, Stud. Surf. Sci. Catal. A 158 (2005) 593–600.
[15] H. Berndt, G. Lietz, J. Völter, Appl. Catal. 146 (1996) 365–379.
[16] A.T. Bell, in: G. Centi, B. Wichterlowa, A.T. Bell (Eds.), Catalysis by Unique Metal Ion Structures in Solid Matrixes, Kluwer Academic Publishers, Dordrecht, 2000, pp. 55–73.
[17] M.J. Rice, A.K. Chakraborty, A.T. Bell, J. Phys. Chem. B 104 (2000) 9987–9992.
[18] B.I. Dunlap, N. Rösch, Adv. Quant. Chem. 21 (1990) 317–339.
[19] T. Belling, T. Grauschopf, S. Krüger, F. Nörtemann, M. Staufer, M. Mayer, V.A. Nasluzov, U. Birkenheuer, A. Hu, A.V. Matveev, A.M. Shor, M.S.K. Fuchs-Rohr, K.M. Neyman, D.I. Ganyushin, T. Kerdcharoen, A. Woiterski, A.B. Gordienko, S. Majumder, N. Rösch, ParaGauss version 3.0, Technische Universität München, 2004.
[20] T. Belling, T. Grauschopf, S. Krüger, M. Mayer, F. Nörtemann, M. Staufer, C. Zenger, N. Rösch, in: H.-J. Bungartz, F. Durst, C. Zenger (Eds.), High Performance Scientific and Engineering Computing; Lecture Notes in Computational Science and Engineering, vol. 8, Springer, Heidelberg, 1999, pp. 441–455.
[21] (a) A.D. Becke, Phys. Rev. A 38 (1988) 3098–3100;
(b) J.P. Perdew, Phys. Rev. B 33 (1986) 8822–8824;
J.P. Perdew, Phys. Rev. B 34 (1986) 7406.
[22] (a) F.B. van Duijneveldt, IBM Res. Rep. (1971) RJ 945;
(b) S. Huzinaga (Ed.), Gaussian Basis Sets for Molecular Calculations, Elsevier, Amsterdam, 1984;
(c) A. Veillard, Theor. Chim. Acta 12 (1968) 405–411;
(d) M.R. Bär, J. Sauer, Chem. Phys. Lett. 226 (1994) 405–412.
[23] S. Huzinaga, J. Chem. Phys. 66 (1977) 4245.
[24] I.V. Yudanov, R. Sahnoun, K.M. Neyman, N. Rösch, J. Chem. Phys. 117 (2002) 9887–9896.
[25] (a) J. Gale, GULP, version 1.3, Imperial College, London, 2001;
(b) J.D. Gale, J. Chem. Soc., Faraday Trans. 93 (1997) 629–637.
[26] V.A. Nasluzov, E.A. Ivanova, A.M. Shor, G.N. Vayssilov, U. Birkenheuer, N. Rösch, J. Phys. Chem. B 107 (2003) 2228–2241.
[27] E.A. Ivanova Shor, A.M. Shor, V.A. Nasluzov, G.N. Vayssilov, N. Rösch, J. Chem. Theory Comput. 1 (2005) 459–471.
[28] (a) G.N. Vayssilov, A. Hu, U. Birkenheuer, N. Rösch, J. Mol. Catal. A 162 (2000) 135–145;
(b) G.N. Vayssilov, J.A. Lercher, N. Rösch, J. Phys. Chem. B 104 (2000) 8614–8623;
(c) J.F. Goellner, B.C. Gates, G.N. Vayssilov, N. Rösch, J. Am. Chem. Soc. 122 (2000) 8056–8066;
(d) G.N. Vayssilov, N. Rösch, J. Am. Chem. Soc. 124 (2002) 3783–3786;
(e) K.M. Neyman, G.N. Vayssilov, N. Rösch, J. Organomet. Chem. 689 (2004) 4384–4394;
(f) G.N. Vayssilov, B.C. Gates, N. Rösch, Angew. Chem. Int. Ed. 42 (2003) 1391–1394.
[29] X.F. Wang, L. Andrews, J. Phys. Chem. A 108 (2004) 11006–11013.
[30] V.A. Macrae, T.M. Greene, A.J. Downs, Phys. Chem. Chem. Phys. 6 (2004) 4586–4594.
[31] Note that these experimental values may be affected by interaction with a rare-gas matrix, but at present we are not are not able to reliably estimate these effects.
[32] A. Görling, S.B. Trickey, P. Gisdakis, N. Rösch, in: J. Brown, P. Hofmann (Eds.), Topics in Organometallic Chemistry, 4, Springer, Heidelberg, 1999, pp. 109–165.
[33] L.A.M.M. Barbosa, G.M. Zhidomirov, R.A. van Santen, Catal. Lett. 77 (2001) 55–62.
[34] N.A. Kachurovskaya, G.M. Zhidomirov, R.A. van Santen, Res. Chem. Intermed. 30 (2004) 99–103.
[35] J. Penzien, A. Abraham, J.A. van Bokhoven, A. Jentys, T.E. Müller, C. Sievers, J.A. Lercher, J. Phys. Chem. B 108 (2004) 4116–4126.